Preflashover mass spectrometry*

J. A. Panitz
Sandia Laboratories, Albuquerque, New Mexico 87115
(Received 14 August 1972)

A bakeable time-of-flight mass spectrometer has been combined with a novel probe assembly in order to directly investigate the ion species formed prior to and during the flashover of an ultrahigh-vacuum diode. Species are identified by their known kinetic energy and the time correlation between their arrival at a detector and a high-voltage pulse applied to the cathode of the diode. By varying the ratio of the pulse amplitude to a positive bias applied to the anode, the extent of ion production in the gap can be probed. Observations at 300 °K and 10^{-9} Torr indicate the presence of both highly charged metal anode ions and adsorbed residual gas prior to flashover. No detected species were formed in the gap, in contrast to what was expected from the results of Davies and Biondi. It is suggested that the absence of such ions may be related to the magnitude of the macroscopic field in the gap, since preliminary observations at flashover show a noticeable change in the nature and abundance of ion species. Electron-induced desorption appears to be the primary preflashover production mechanism, although field-enhanced desorption may also be significant.

I. INTRODUCTION

The study of high-voltage flashover phenomena in vacuum has occupied the literature for many decades.[1,2] Although much information has accumulated from measurements of current and voltage,[3-5] the mechanism responsible for the formation and propagation of the spark is not well understood. Recent mass spectrometer observations of ion species formed during flashover[6] have only confirmed the complexity of the process.

It is the purpose of the preflashover spectrometry technique[7] to investigate for the first time, and with single-particle sensitivity, the nature of the species formed *prior* to flashover at the anode surface or in the gap between the electrodes. The positive identification of these species is necessary to elucidate the nature of the formative mechanism. It is essential in deciding which of the most probable processes, either electron-induced desorption or field-induced desorption, at the anode surface is responsible for ion formation. Granting the existence of cathode microprotrusions which act as field electron emitters,[8] one might also expect anode protrusions with local fields sufficiently large to cause field desorption of residual gas or thermally enhanced field evaporation of the emitters, resulting in the formation of characteristic highly charged metal anode ions.

II. THEORY

During operation, a bias potential V_B is applied to the anode of the vacuum diode. When a high-voltage pulse[9] $-V_P$ is applied to the cathode, ions formed at the anode surface or in the gap of the diode are accelerated and pass into a drift region at ground potential through photoetched apertures in the cathode. Initially, a single 0.5-mm-diam hole was used to sample the ions, but poor collection statistics and the desire to maintain a uniform field at the anode surface necessitated the more elaborate configuration shown schematically in Fig. 1. An einzel lens at the entrance to the drift region focuses the ions on an electron multiplier 1 m away. The time interval between the resulting signal, displayed on an oscilloscope, and the beginning of its sweep, triggered by the pulse applied to the cathode, is a direct measure of the ion's travel time. If the amplitude of the cathode pulse remains constant for a time longer than the ion's travel time in the acceleration region and if the ion's initial kinetic energy is zero, its final kinetic energy will be just

$$\tfrac{1}{2}mv_F^2 = neV_B[1-(d/D)(1+V_P/V_B)]$$

$$0 \le (d/D)(1+V_P/V_B) \le 1.0, \quad (1)$$

where m is the ion's mass, v_F its velocity at the entrance to the drift region, ne its charge, d the distance from its formation position to the anode, D the gap spacing, and V_P the magnitude of the applied negative pulse. Since the ion's travel time in the gap and lens is short compared to its travel time in the drift region, its total travel time T is, to a very good approximation, just

$$T = L/v_F, \quad (2)$$

where L is the length of the drift region, here 1.081 m.

The ion is identified by its mass-to-charge ratio expressed in terms of the applied voltages, the measured travel time, the position of formation, and the known drift distance. Combining Eqs. (1) and (2) gives the desired result:

$$m/n = 0.165V_B[1-(d/D)(1+V_P/V_B)]T^2, \quad (3)$$

where distances are measured in meters, voltages in kilovolts, time in microseconds, and m/n in atomic mass units.

Now consider two identical species: one formed at the

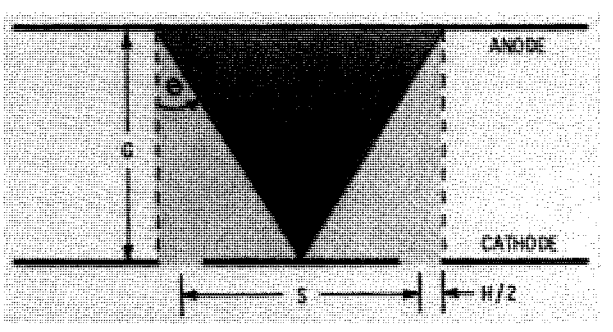

FIG. 1. Electrode details. Typically, $G = 0.5$ mm, $H = 0.05$ mm, $S = 0.5$ mm, the field emission half-angle $\theta = 40°$. Only two of the 300 holes photoetched in the 0.05-mm-thick Be-Cu cathode are shown.

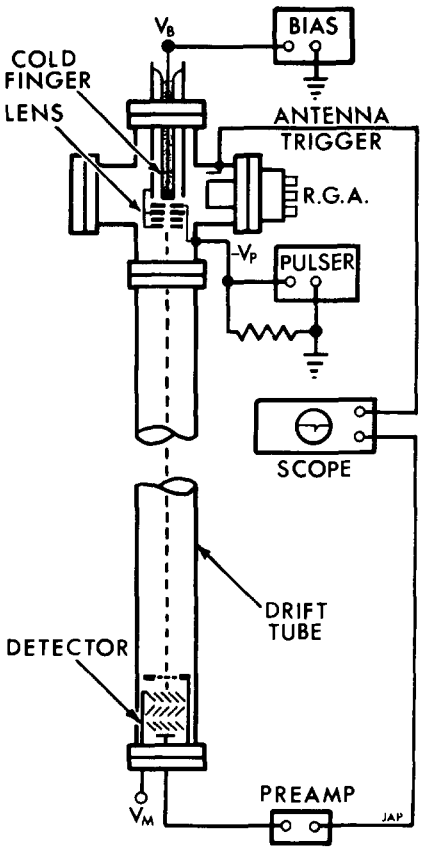

FIG. 2. Preflashover time-of-flight spectrometer.

anode, the other in the gap. For the ion formed at the anode, $d=0$ in Eq. (3) and the observed travel time T becomes independent of the pulse amplitude. Combining the resulting expression for T_{anode} with Eq. (3) solved for T_{gap} and rearranging gives

$$T_{gap}=T_{anode}[1-(d/D)(1+V_P/V_B)]^{-1/2}. \quad (4)$$

Equation (4) indicates that the travel time of the ion produced in the gap will be longer than that of the same ion produced at the anode and will be dependent on its formation position d. Effectively, an ion produced in the gap will acquire less kinetic energy than its counterpart produced at the anode. Therefore, it will travel a longer time in the drift region, appearing as a slower ion or one with a greater m/n.

The reproducibility of the mass-to-charge ratio of a given species is directly proportional to the reproducibility of its formation position in the gap, provided the applied voltages remain constant. Furthermore, to even detect an ion, the inequality of Eq. (1) must be satisfied, that is,

$$0 \leq (d/D)(1+V_P/V_B) < 1.0. \quad (5)$$

Equation (5) suggests that the fraction of the total gap spacing d/D in which ionization occurs can be probed by varying the ratio of the pulse to bias voltage. For example, with $V_P/V_B=3.0$, ions can be detected from the anode surface ($d=0$) to a gap position $d=\frac{1}{4}D$. For $V_P/V_B=\frac{1}{3}$, ions can be detected from the anode to a gap position $d=\frac{3}{4}D$. If the ions were to be produced in maximum number at gap center ($\frac{1}{2}D$), as a recent experiment might suggest,[10] the observed ion current would maximize as the pulse—to—bias-voltage ratio was varied between the above limits.

Using a calibration procedure described previously,[11] the mass-to-charge ratio of a detected species can be determined to better than 1 amu at $m/n=50$ or, in special cases, to better than 0.1 amu for $m/n \leq 3.0$.

III. APPARATUS

Figure 2 is a schematic diagram of the bakeable ultra-high-vacuum time-of-flight mass spectrometer. Trapped oil diffusion and electron-ion pumps allow typical operating pressures of less than 10^{-9} Torr after bakeout at 300 °C. The spectrometer source is a parallel plate vacuum diode composed of a replaceable metal anode and type 304 stainless steel cathode 0.5 cm^2 in area and separated by 0.5 mm. The anode, located at the end of a glass cold finger, can be cooled to cryogenic temperatures, encouraging preferential absorption on its surface when known gases are introduced into the vacuum system.

The high-voltage pulse is supplied by a properly terminated commercial pulse generator[12] of high output impedance. The pulse amplitude is adjustable from 0 to 35 kV, and has a rise time of 10 nsec and a width of 100 nsec. A small in-vacuum antenna and emitter follower preamp detect the arrival of the pulse at the cathode, providing a zero reference for travel time measurements, as well as a signal to initiate the time-measuring sequence.

The bias voltage, which uniquely determines an anode ion's kinetic energy, is set by a precision high-voltage power supply,[13] with a ripple of less than 250 mV and a regulation of better than 0.0025% at 20 kV.

Species are detected with a focused mesh electron multiplier[14] operated at a gain of 10^6. A grounded grid placed 2 mm in front of its first dynode defines the extent of the drift region and insures that the ion's travel time in the acceleration region in front of the multiplier is negligible.

IV. OBSERVATIONS AND CONCLUSIONS

Although the pulse—to—bias-voltage ratio was varied in these experiments, the sum of the bias voltage and the pulse applied to the cathode was held constant. The resulting field, equal to 5×10^5 V/cm, was approximately 5% below that required for visible flashover. Figure 3 is a photograph of several typical oscilloscope time sweeps. The identical travel times in successive sweeps indicate a unique ion species.[15] The accuracy in determining a single ion travel time, ±20 nsec, corresponds to a fractional uncertainty in formation position for a given species, $\Delta d/d$, of 1%. For the maximum ratio of pulse to bias voltage used and the known gap spacing, the minimum extent of the ionization region can be determined from Eq. (5) to be $d=25$ μ, corresponding to an uncertainty in formation position of $\Delta d=0.25$ μ.

As the pulse amplitude is changed, the observed travel times remain constant, changing only with a change in the applied bias voltage V_B. This indicates that the

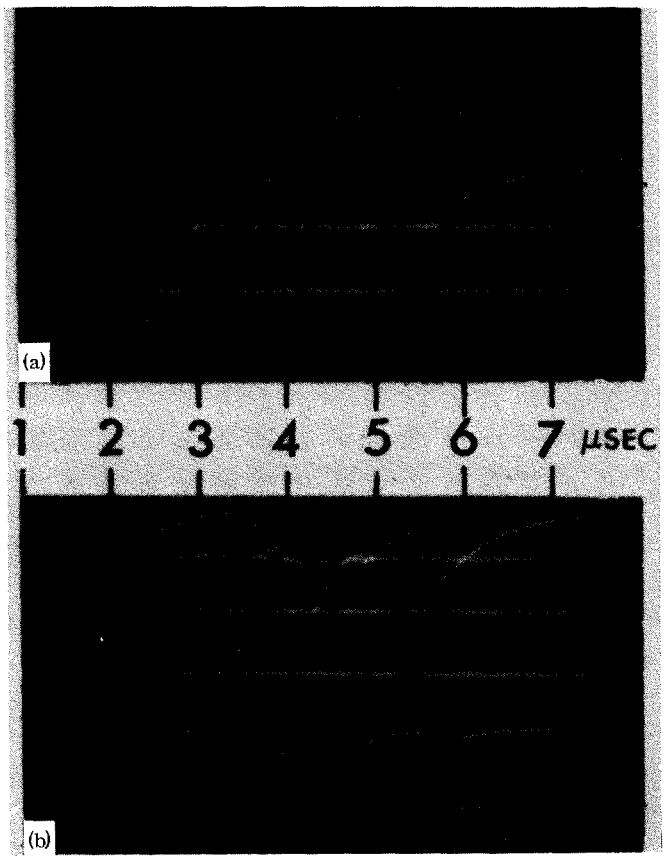

FIG. 3. Ion travel times, $V_B = 6$ kV, $V_P = 13$ kV (a), $V_P = 12$ kV (b). The arrival of an ion produces a negative pulse from the electron multiplier. Typical ion current per time sweep is estimated at 10^{-9}—10^{-14} A.

species are being formed at the anode. In Fig. 4(a), the corresponding mass-to-charge ratios [calculated from Eq. (3) with $d = 0$] are displayed in histogram form. Figure 4(b) shows the corresponding residual gas spectra[16] taken in the same system and plotted as a histogram, normalized to the H^+ peak of Fig. 4(a). The excellent agreement of m/n values between the two histograms for known residual gas species indicates that the equation used to determine the species in 4(a) is valid; that is, the assumption of ion formation at the anode is correct. Furthermore, the comparison shows that absorbed gas ions from the anode, as well as metal anode ions, form the preflashover ion currents. The hydrocarbon species are produced by the diffusion pumped system used during preliminary evacuation of the spectrometer. Their presence indicates that even with careful trapping (in this case, a chilled water baffle and constant level nitrogen trap) contamination of the electrodes is a problem, although the system was baked and maintained at pressures less than 10^{-9} Torr. It appears that unless a clean flashover experiment is performed, observations of electrode conditioning and claims that certain phenomena are independent of pressure will have to be reviewed critically. It is now apparent that outgassing of the electrodes can provide local contaminant pressures at their surface significantly different than those indicated by remote gauges.

A close examination of the individual data points shows that the species between $m/n = 13$ and $m/n = 14$ in Fig. 4(a) actually peak at $m/n = 13.5$ corresponding to Al^{2+}. Interestingly, a negligible amount of Al^{1+} was observed, in agreement with results obtained at flashover.[17] Of particular interest is the absence of species between $m/n = 22$ and 24 and $m/n = 30$ and 34 in the residual gas spectra, but present in the preflashover spectra reflecting the use of an alloy anode.[18] Conversely, the absence of a peak at $m/n = 28$ in the preflashover spectra and the large peaks at $m/n = 12$ and $m/n = 16$ indicates that CO is dissociating at the anode surface during the preflashover process. A detailed study of the individual peaks below $m/n = 3.0$ shows that H_3^+ and H_2^+ are dissociating in the high electric field near or at the anode surface. The presence of such processes is not surprising since the macroscopic field in the gap is sufficient, even without electron bombardment of the anode,[19,20] to cause field dissociation of these species.[21,22]

Figure 4(a) plots the data obtained for all ratios of pulse to bias voltage used, between approximately 0.33 and 19.0, for constant field strength in the gap. This corresponds to a variation in the extent of the ionization region from $d = 3D/4$ to $d = D/20$. If the abundance of an individual species is examined as a function of increasing voltage ratio or decreasing ionization region, no noticeable discontinuities are observed. This further indicates that ionization is taking place at the anode surface and not in the gap, at least to within the previously mentioned uncertainty of 0.25 μ. It is interesting to note that with the possible exception of the residual gas constituents, the species observed are similar, at least in charge state, to those reported for refractory metals in the classic atom-probe experiments of Müller and co-workers.[23,24] This may suggest that field-induced desorption is contributing to the production of preflashover ion species, although it is still reasonable to expect that electron-induced desorption is the primary production mechanism.

In view of the previous results of Davies and Biondi,[10] it is perhaps surprising that no measurable number of ions was observed as originating in the gap itself. Their observation of neutral electrode material in the gap microseconds before flashover would suggest that corre-

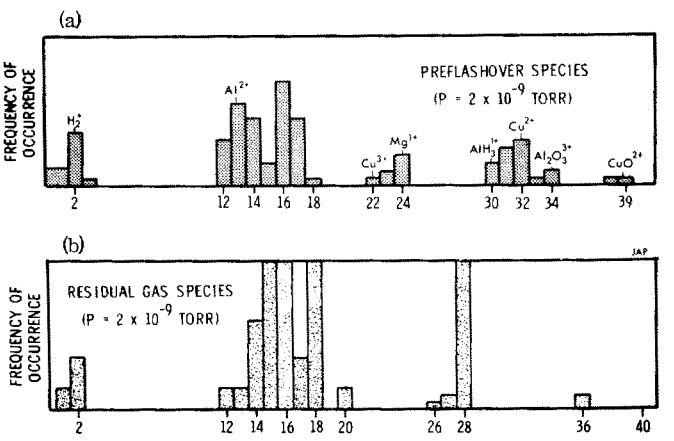

FIG. 4. (a) Preflashover species, (b) residual gas species.

sponding ion species should be observed, formed by electron bombardment from the cathode. Preliminary observations have been made as the field in the gap is increased to the value at which visible flashover occurs. A definite increase of several orders of magnitude in the abundance of anode species occurs, whose initial kinetic energy and energy distribution is appreciable. Fast neutrals or metastables have also been observed. This in turn suggests that field-dependent processes are occurring and that the occurrence of ion production in the gap may be closely related to the value of the macroscopic field.

ACKNOWLEDGMENTS

The author wishes to express his thanks to R. L. Park and R. L. Schwoebel for many helpful discussions, J. E. Boers for his aid in the computer simulation of einzel lens properties, and D. W. Tipping for technical assistance.

---

*Work supported by the U. S. Atomic Energy Commission.

[1]R. W. Wood, Phys. Rev. **5**, 1 (1897).
[2]G. A. Mesyats, S. P. Bugayev, D. I. Proskurovskiy, V. I. Eshkenazi, and YA. YA. Yurike, Radio Eng. Electron. Phys. **14**, 1919 (1969).
[3]H. Boersch, H. Hamish, and W. Ehrlich, Z. Angew. Phys. 15, 518 (1963).
[4]R. Hackam and S. K. Slaman, Proc. IEEE **119**, 377 (1972).
[5]H. S. Powell and P. A. Chatterton, Vacuum **20**, 419 (1970).
[6]E. D. Korop and A. A. Plyutto, Sov. Phys.-Tech. Phys. **15**, 1986 (1971).
[7]J.A. Panitz, Proceedings of the Fifth International Symposium on Discharges and Electrical Insulation in Vacuum, Poland, 1972 (unpublished).
[8]R. N. Bloomer and B. M. Cox, Vacuum **18**, 379 (1968).
[9]The sum of the bias voltage and pulse amplitude is adjusted so that the field in the gap is a few percent below that required for visible flashover. Therefore, preflashover conditions are always maintained during each applied pulse.
[10]D. K. Davies and M. A. Biondi, J. Appl. Phys. **41**, 88 (1970).
[11]J. A. Panitz, S. B. McLane, and E. W. Miller, Rev. Sci. Instrum. **40**, 1321 (1969).
[12]Electro-Optical Instruments, Inc., Pasadena, Calif. model CU/60/A.
[13]Power Designs, Inc., Palo Alto, Calif., model 1584R.
[14]Johnston Laboratories, Inc., Cockeysville, Md., model MM-1.
[15]Actually, identical travel times are also possible for two different ions formed in different locations in the gap such that
$$(m/n)_1[1-(d_2/D)(1+V_P/V_B)] = (m/n)_2[1-(d_1/D)(1+V_P/V_B)].$$
However, repeated identical travel times would imply two unique formation positions in the gap for two unique species, which is highly improbable.
[16]Granville-Phillips Corp., Boulder, Colo., SpectraScan-400 residual gas analyzer.
[17]J. T. Grissom and J. C. Newton, in Ref. 7.
[18]Aluminum alloy 2024 condition T351. Primary constituents: Al (91.4–93.7%), Cu (3.8–4.9%), Mg (1.2–1.8%), all others less than 1%.
[19]T. E. Madey and J. T. Yates, Jr., J. Vac. Sci. Technol. **8**, 525 (1971).
[20]I. Newsham, J. V. Hogue, and D. R. Sandstrom, J. Vac. Sci. Technol. **9**, 596 (1972).
[21]J. R. Hiskes, Phys. Rev. **22**, 1207 (1961).
[22]H. Wind, Nucl. Fusion **6**, 67 (1961).
[23]E. W. Müller, J. A. Panitz, and S. B. McLane, Rev. Sci. Instrum. **39**, 83 (1968).
[24]E. W. Müller, Naturwissenschaften **57**, 222 (1970).